SUPPORTING INFORMATION APPENDIX

SI Results and discussion

Identification of coumaphos resistance, in a *Varroa* population for the Aegean island Andros

Among several populations tested with a coumaphos diagnostic dose of 200 mg a.i./L, which caused approximately 95% mortality in the ATH-S population, the AN-CR population from the Aegean island Andros exhibited substantially reduced mortality rates (7%) compared to other populations tested (Table S1). This Andros population originated from a beekeeper who used coumaphos almost exclusively for many years.

Acaricide uptake/penetration is not involved in resistance

Acaricide uptake (penetration) was analysed by comparing ^{14}C coumaphos internalization between the AN-CR and the ATH-S populations after (tarsal) sublethal exposure on coated bioassay vials. The internalization of ^{14}C coumaphos was approximately 10% (internal cpm/total cpm) over the time span of the experiment for both populations and not significantly different between resistant and susceptible mites (Table S2), indicating that reduced penetration is not involved in resistance.

Identical carboxyl/choline esterases profile between resistant and susceptible *Varroa*

Total protein extract was used to profile general esterase hydrolytic activity against 1-NA after separation by IEF 3 – 10 (Figure S1). Several bands displayed esterase activity, all in the zone between pI 6.0 and 4.5 and the profile was identical between the two populations ATH-S and AN-CR (Figure S1), indicating that carboxyl/choline esterases are not involved in resistance.

***Varroa* transcriptome analysis and honey bee viruses**

After filtering the RNAseq dataset (Table S3) for the presence of viral sequences (Table S4), a total of 42.4, 59.1 and 45.2 million Illumina paired-end reads were obtained for ATH-S, AN-CR and tAN-CR, respectively. Alignment of the filtered RNA-seq reads against the *V. destructor* genome resulted in an overall mapping rate of uniquely mapped reads of 86.7 ± 1.7 SE% across samples (Table S4). A PCA revealed that 51.7% of the total variation could be explained by principal component 1 (PC1) while 19.4%

could be explained by PC2. Replicates clustered by resistance phenotype, regardless of coumaphos exposure in the AN-CR and tAN-CR populations (Figure S2). A differential gene expression analysis was subsequently performed between the AN-CR and the ATH-S population and between the coumaphos treated tAN-CR population and the AN-CR population. A total of 270 DEGs were identified in AN-CR compared to ATH-S (fold change (FC) > 2 and a Benjamini-Hochberg adjusted p-value < 0.05) (Dataset S2). Twenty-eight DEGs were differentially overexpressed, whereas 242 were underexpressed. Only one gene was differentially expressed in the pairwise comparison between the tAN-CR and AN-CR populations (cytb; $\log_2$FC of 1.03, Dataset S2).

SI Materials and Methods

Mite populations

Varroa mites from infested *A. mellifera* hives were collected from six different locations in Greece (Athens, Thessaloniki, Sparti, Crete, Andros, Naxos), based on the history of acaricide applications and indications of treatment failures reported by beekeepers. From each analyzed hive and location, brood frames were collected, brood cells uncapped and *Varroa* mites that were either on the bee larvae or in the inner surface of the bee brood cell were collected in an Eppendorf tube using a fine paintbrush.

Diagnostic bioassays

Chemicals dissolved in acetone were freshly prepared at different concentrations and 0.5 mL of solutions was placed into individual 12-mL glass vials. Vials were rolled until the acetone evaporated, leaving a uniform film of acaricide on the inner surface of the vials. Batches of ten (10) adult female mites were introduced into the coated vials, closed with holed parafilm, each time at 25 °C for 20 h. Diagnostic assays based on the LC_{95} of the ATH-S were conducted.

Penetration rate of ^{14}C coumaphos.

The penetration rate of ^{14}C coumaphos in *Varroa* populations was determined according to Balabanidou et al (2016) (1) with slight modifications. Briefly, pools of 5-10 female *Varroa* mites were exposed to [^{14}C] coumaphos coated bioassay vials at approximately LC_5 for each population at 2 h for 25°C. Subsequently, they were rinsed

three times with 200 μl methanol and homogenized in pools of 10 in 200 μl methanol. Ten milliliters of liquid Scintillation Counting Mixture (Ultima Gold; 6013326; PerkinElmer) were added to each sample and the corresponding counts per minute were measured on a beta counter (LS1701; Beckman). The penetration rate (PR) was calculated as the ratio of internal counts per minute to total counts per minute.

Isoelectric focusing polyacrylamide analysis (IEF)

Isoelectric focusing (IEF) on polyacrylamide gels was performed for the separation of CCEs, as previously described (2). IEF was conducted with an Xcell Surelock Mini-Cell (Invitrogen, Groningen, The Netherlands) using precast IEF (5% polyacrylamide) gels with immobilized pH gradient in the pH ranges 3-10 and 3-7. Gels and samples (10μg protein extract) were prepared and run according to the manufacturer's instructions. CCEs were visualized with 1-naphthyl acetate (1-NA) and Fast blue RR.

Quality control and PCA analysis of RNAseq data

The quality of the reads was verified using FASTQC version 0.11.5 (3). Sixteen out of twenty-four FASTQ files gave a warning for overrepresented sequences and a BLASTn search against the NCBI non-redundant nucleotide database showed that the majority of these overrepresented sequences had a best BLASTn hit with honeybee virus sequences. Subsequently, viral contamination was removed by aligning the generated reads to a selection of 19 bee virus genomes (Table S2) using STAR 2.5.0a, (4) and retaining the unmapped reads for subsequent analyses. Bee virus filtered reads were aligned to the *V. destructor* genome (GenBank: GCA_002443255.1) (5) using the two-pass alignment mode of STAR 2.5.0a (4) with a maximum intron size set to 20kb. Read counts per gene were obtained using the default settings of HTSeq 0.6.0 (6) with the "STRANDED" flag set to "reverse", the "feature type" flag set to "exon", the "id" flag set to "gene" and the *Varroa* genome annotation (GCF_002443255.1_Vdes_3.0_genomic.gff, 10247 nuclear + 13 mitochondrial protein coding genes). A PCA was created as described by Love et al 2015 (7). Briefly, read counts were first normalized using the regularized-logarithm (rlog) transformation implemented in the DESeq2 R-package (8). A PCA was then performed using the R-packages stats (version 3.5.2) and ggplot2 (version 3.1.0) with the 1000 most variable genes across all RNA-seq samples (Figure S2).

SI References

1.   V. Balabanidou, *et al.*, Cytochrome P450 associated with insecticide resistance catalyzes cuticular hydrocarbon production in *Anopheles gambiae*. *Proc. Natl. Acad. Sci* . **113**, 9268–9273 (2016).

2.   T. Van Leeuwen, S. Van Pottelberge, L. Tirry, Comparative acaricide susceptibility and detoxifying enzyme activities in field-collected resistant and susceptible strains of *Tetranychus urticae*. *Pest. Manag. Sci.* **61**, 499–507 (2005).

3.   S. Andrews, FastQC: a quality control tool for high throughput sequence data (2010).

4.   A. Dobin, *et al.*, STAR: ultrafast universal RNA-seq aligner. *Bioinformatics* **29**, 15–21 (2013).

5.   M. A. Techer, *et al.*, Divergent evolutionary trajectories following speciation in two ectoparasitic honey bee mites. *Communications Biology* **2**, 357 (2019).

6.   S. Anders, P. T. Pyl, W. Huber, HTSeq--a Python framework to work with high-throughput sequencing data. *Bioinformatics* **31**, 166–169 (2015).

7.   M. I. Love, S. Anders, V. Kim, W. Huber, RNA-Seq workflow: gene-level exploratory analysis and differential expression. *F1000Res* **4**, 1070 (2015).

8.   S. Anders, *et al.*, Count-based differential expression analysis of RNA sequencing data using R and Bioconductor. *Nat Protoc* **8**, 1765–1786 (2013).
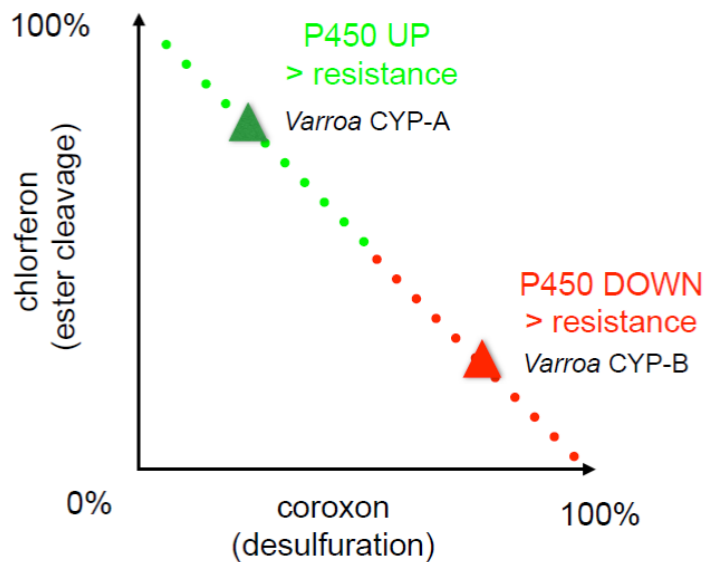
SI Figures
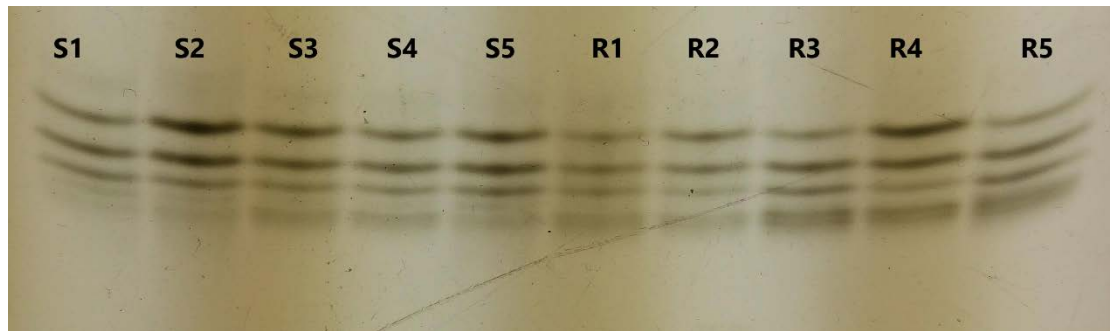
Figure S1. Isoelectric focusing polyacrylamide analysis (IEF) for the separation of carboxyl/choline esterases (CCEs). IEF was conducted with an Xcell Surelock Mini-Cell using precast IEF (5% polyacrylamide) gels with immobilized pH gradient in the pH ranges 3-10 and 3-7. Gels and samples (10µg protein extract) were prepared and run according to the manufacturer's instructions. Esterases isozymes between five Susceptible ATH-S (S1-S5) mites and five Resistant AN-CR (R1-R5) mites after separation with IEF pH 3-7, visualized with 1-NA activity staining.
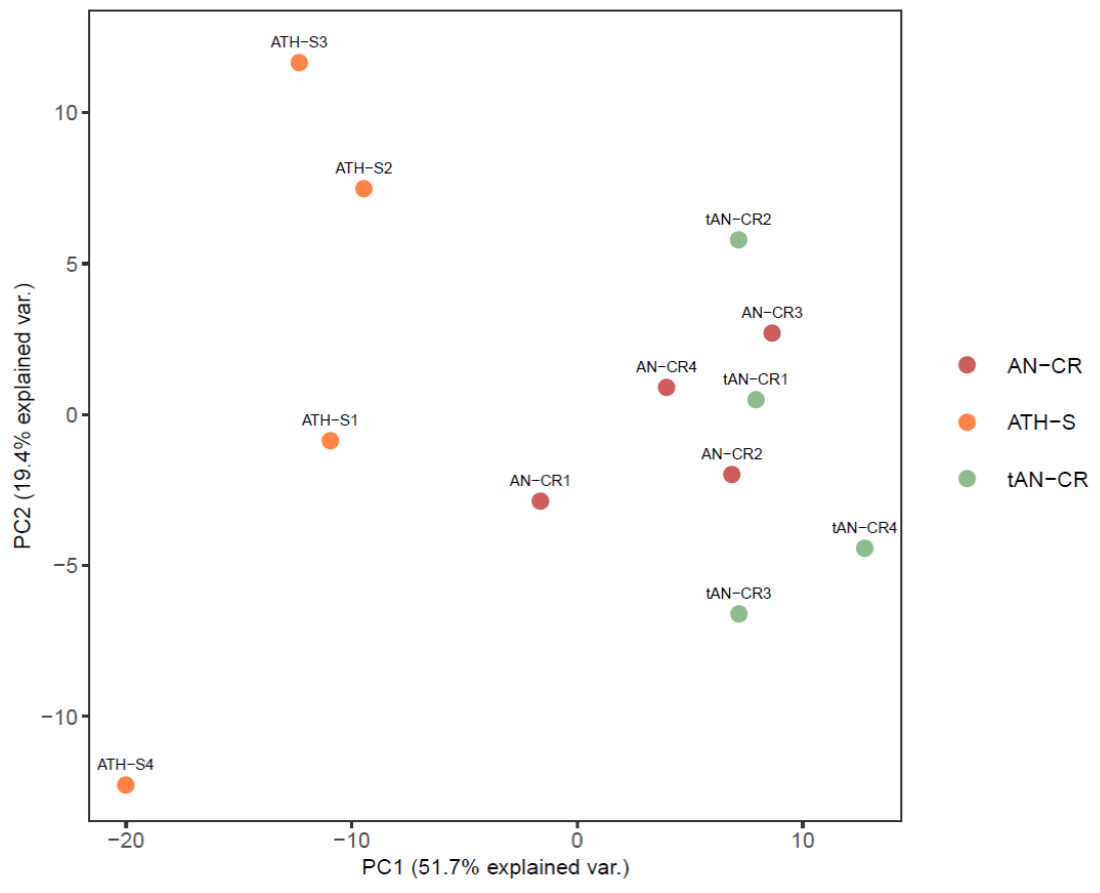
Figure S2. Principal component analysis (PCA). Gene expression relationships among *V. destructor* populations/treatments; coumaphos susceptible *V. destructor* population (ATH-S), coumaphos resistant *V. destructor* population (AN-CR) and coumaphos resistant *V. destructor* population treated with 200 mg a.i. coumaphos/L aceton (tAN-CR).

Figure S3. The Janus face of P450 metabolism of coumaphos. P450 enzymes can metabolize either the chloromethylcoumarinyl group, or the phoshorothioate (P=S) moiety. The latter reaction leads to two major products in proportions that are dependent on each P450 enzyme. The figure shows that the global P450 metabolism of the coumaphos P=S group in an organism, as well as of each P450 enzyme, is therefore located on the stippled line. All other factors being equal (tissue distribution, developmental expression), both up- or down-regulation of the P450 enzymes can theoretically lead to resistance. In this schematic example, up-regulation of CYP-A would increase ester cleavage (detoxification) more than desulfuration, while down-regulation of CYP-B would decrease desulfuration (activation to an AchE inhibitor) more than ester cleavage.

SI Tables

Table S1. Percentage mortality of *Varroa* populations in response to coumaphos diagnostic dose (DD).

Population	Date	n	Mortality (%)	Number of applications (5y)	Global Positioning System coordinates (N,E)
Athens (AUA-S)	7/2017	80	93±4	-	(37.982475, 23.705533)
Andros (AN-CR)	9/2017	60	7±3	C (10x)	(37.861864, 24.790071)
Sparti	7/2018	60	88±3	A (6x),F(4x)	(36.846375, 23.001934)
Naxos	9/2017	60	62±3	C (5x),F(3x),A(2x)	(37.099604, 25.482232)
Crete	9/2018	60	90±4	A (5x),F(4x),C(1x)	(35.284983, 25.062404)
Thessaloniki	7/2019	60	82±3	A (5x),C(2x),O(3x)	(40.579336, 23.046397)

n: number of mites tested (in batches of 10);
DD: Diagnostic dose of 200 ppm, in 500ul used per vial;
C: coumaphos; A: Amitraz; F: tau-Fluvalinate

Table S2. Penetration Ratio of ^{14}C Coumaphos in coumaphos resistant (AN-CR) and susceptible (ATH-S) *Varroa* mites.

Strain	PR(10^{-2}), (±SD)	P value
ATH-S	9.85 (±0.39)	0.219
AN-CR	10.35 (±0.45)	

n=3 biological replicates.

PR. Penetration Rate: ratio of internal counts per minute to total counts per minute; SD: Standard Deviation. Statistical analysis was performed with the independent samples t-test.

Table S3. Mapping rates of the strand-specific paired-end Illumina reads against the
V. destructor genome.

	Uniquely mapped reads (%)	Number of uniquely mapped reads	Averaged mapped length	Reads mapped to multiple loci	Reads unmapped too short (%)	Reads mapped to viral sequences
ATH-S1	81.75	5027037	248.7	112374	16.31	8338159
ATH-S2	70.83	13257087	248.61	258171	27.70	8134
ATH-S3	90.44	11533243	248.75	248464	7.49	2242060
ATH-S4	93.52	12567678	248.71	283439	4.23	3741
AN-CR1	85.39	15008441	248.58	354428	12.50	2697507
AN-CR2	88.27	13756632	248.67	391407	9.14	3881935
AN-CR3	87.60	14181859	248.61	450747	9.56	1289973
AN-CR4	88.52	16113546	248.46	358375	9.45	126384
tAN-CR1	89.88	12679321	248.84	308727	7.88	6515057
tAN-CR2	88.26	11095579	248.76	339215	8.98	3933592
tAN-CR3	88.73	13710691	248.69	286356	9.36	212792
tAN-CR4	87.23	7735415	248,77	241339	10.01	7593504

Table S4. List of honey bee viruses and their accessions used to filter/align the FASTQ files with the STAR software (version: 2.5.3), using the two-pass alignment mode and the --outReadsUnmapped Fastx option. Unmapped reads were retained for the subsequent transcriptomic analyses.

Viruses	Accession
Acute bee paralysis virus	NC_002548.1
Apis rhabdovirus	KY354230.1
Apis bunyavirus	KY354236.1, KY354237.1
Apis dicistrovirus	KY354239.1
Apis flavirus	KY354238.1
Apis noravirus	KY354240.1
Bee Macula like virus	NC_027631.1
Black queen cell virus	NC_003784.1
Chronic bee paralysis virus	NC_010711.1
Deformed wing virus	NC_004830.2, KT733632.1, KT733627.1, KT733619.1
Israeli acute paralysis virus	NC_009025.1
Kakugo virus	AB070959.1, AB245506.1, KT733624.1, AB251935.1
Kashmir bee virus	NC_004807.1
Lake Sinai virus	KY354242.1, KY354241.1, KY354244.1
Moku virus	NC_031338.1
Sacbrood virus	NC_002066.1
Slow bee paralysis virus	NC_014137.1
Varroa destructor virus	NC_006494.1
Varroa tymo virus	NC_027619.1

Table S5. List of primers used in the study

Gene	Forward Primer sequence (5' →3')	Reverse Primer sequence (5' →3')	Product size	Reaction Eficiency
RT-qPCR primers				
18S rRNA (LOC111253957)	AATGCCATCATTACCATCCT	CAAAAACCAATCGGCAATCT	60 bp	99.91%
NADH dehydrogenase (LOC111249888)	TCCGCTTAAGGAGCTTATCG	ATCACGCACAGCAGGTTATC	72 bp	100.6%
CYP4EP4 (LOC111248731)	CACGCACGGTCACAAAAGAG	CGGAAGAAAGCGGTCAGGAT	143 bp	99.17%
CYP3012A6 (LOC111246534)	CTTCAGCTTTGGGCCTCGTA	TCCGGTGTGTTGACGAGTTT	147 bp	95.22%
dsRNA synthesis primers*				
dSGFP	<u>TAATACGACTCACTATAGGGAGA</u>ACGTAAACGGCCACAAGTTC	<u>TAATACGACTCACTATAGGGAGA</u>CTTGTACAGCTCGTCCATGCC	600 bp	
dSCYP4EP4	<u>TAATACGACTCACTATAGGGAGA</u>GCCTTGGACTGCTAACAAGC	<u>TAATACGACTCACTATAGGGAGA</u>CCTGCAAGTCTGCCTACTGT	417 bp	
dSCYP3012A6	<u>TAATACGACTCACTATAGGGAGA</u>GTGGAATTGCCTTCGTCTGC	<u>TAATACGACTCACTATAGGGAGA</u>TCGTATCTGCGCCTCCTAGT	441 bp	

* Part of the sequence (underlined) represents the T7 promoter for dsRNA synthesis

Dataset S1 - *De novo* transcriptome assembly of Varroa destructor (CLC Genomics Workbench 11) described in this study.

Dataset S1 can be downloaded from the following link:

https://drive.google.com/file/d/1-Z8gC9EO2Ophg8aqvaBoey_mfLj8CyOK/view?usp=sharing

Dataset S2 Differentially expressed genes (DEGs) (log2FC > 1 and Benjamini-Hochberg adjusted p-value <0.05) between the pairwise comparisons of *V. destructor* populations/treatments. AN-CR vs ATH-S (Worksheet1), tAN-CR vs ATH-S (Worksheet2) and tAN-CR vs AN-CR (Worksheet3). Worksheet 4 and 5 contain the shared over- and underexpressed DEGs between the AN-CR vs ATH-S and tAN-CR vs ATH-S comparisons, respectively.

Dataset S2 can be downloaded from the following link:

https://drive.google.com/file/d/1woJoPjy5ChpjwmgvU6pbwUqKeKrUACtK/view?usp=sharing